International Journal of Mass Spectrometry and Ion Processes 126 (1993) 101–114
0168-1176/93/$06.00

Molecular fragmentation and formation processes in plasma desorption mass spectrometry[1]

E.R. Hilf[a,*], W. Tuszynski[a], B. Curdes[a], J. Curdes[a], M. Wagner[b], K. Wien[b]

[a]*Fachbereich Physik, Carl von Ossietzky-Universität, D-2900 Oldenburg, Germany*
[b]*Institut für Kernphysik, T. H. Darmstadt, D-6100 Darmstadt, Germany*

(Received 25 November 1992; accepted 5 January 1993)

Abstract

Molecular fragmentation and formation processes in PDMS are studied by measuring and discussing positive and negative ion spectra of pure carbon or hydrocarbon compounds. Calculations of the hydrodynamic adiabatic expansion of the material from the inner track result in the formation of carbon clusters in agreement with the negative ion spectra. A universal pattern in the negative ion spectra can thus be explained. Results of molecular breakup calculations are compared with the observed positive ions which are assumed to be from the ultratrack. From the comparison we conclude that the breakup of the carbon bonds is entropic and takes place during the desorption while the main part of the hydrogen separation occurs afterwards.

Key words: Plasma desorption mass spectrometry; Fullerenes; β-Carotene; Alkanes; Desorption; Aggregation.

1. Introduction

The discovery of fast, heavy ion induced desorption opened a new field in research and chemical analysis [1,2]. The physics of the process is basically well understood as a fast and violent non-equilibrium process leading to a gentle desorption. Because of the high initial energy densities involved, Macfarlane and co-workers [1,2] originally thought of the mechanism as a plasma that might be formed along the track, which then might relax by blowing away and adiabatically cooling the atoms. Thus he named the process plasma desorption mass spectrometry (PDMS) which became generally accepted, although it became clear, finally by quantitative calculations [3], that the bulk of the material stems from areas far away from the track. The energy is transferred mostly by charge-neutral electronic excitation and finally by mechanical coherent relaxation of the solid (mechanical shock). By this process, the usually large number of desorbed particles, as well as their large kinetic but little internal energy, was finally understood. The process of ionization of the resulting desorbed particles is rather rare despite the huge number of electrons initially set free (see ref. 3).

In the following we present, analyze and interpret positive and negative ion spectra of fullerenes, β-carotene, and some alkanes where negative molecular and fragment ions are not observed by PDMS [4]. For the alkanes a more detailed study is in preparation [5].

The experimental spectra are complemented by

*Corresponding author.
[1]Paper presented at the 6th Texas Symposium on Mass Spectrometry, Gaspé Que., Canada, 15–19 June, 1992.

model calculations. For the fragmentation of molecules in the outer zone we applied the program CRUNCHER [6] assuming an entropic breakup of the molecule. For the process in the inner part of the desorption zone we did a hydrodynamical calculation of a plasma relaxing into the vacuum by adiabatic expansion. The material is assumed to be totally atomized and to then recombine to new molecules and clusters. An analogous process has been well studied in the case of cluster production by expansion of a gas beam through a nozzle [7,8].

Thus, finally the name plasma desorption proposed for the PDMS process by Macfarlane and co-workers comes back to life for the inner part of the desorption area.

2. Experimental

The PDMS spectra of β-carotene and fullerenes were recorded in Oldenburg by the spectrometer OLDA 1 which was built in close cooperation between the two groups in Oldenburg and Darmstadt. OLDA 1 is a linear TOF instrument equipped with an 80 cm flight tube, a 10 μm ^{252}Cf-source, two double stage multichannel plates for start or stop signals, and a time digital converter CTM/M2 connected with a DMI-card, both from Y. LeBeyec, IPN Orsay. The mass resolution is about 700. The operating voltage was ±14 kV, the run time 15 min with β-carotene and 300 min with fullerenes. The β-carotene and fullerene samples were prepared by spraying 15 μl of a

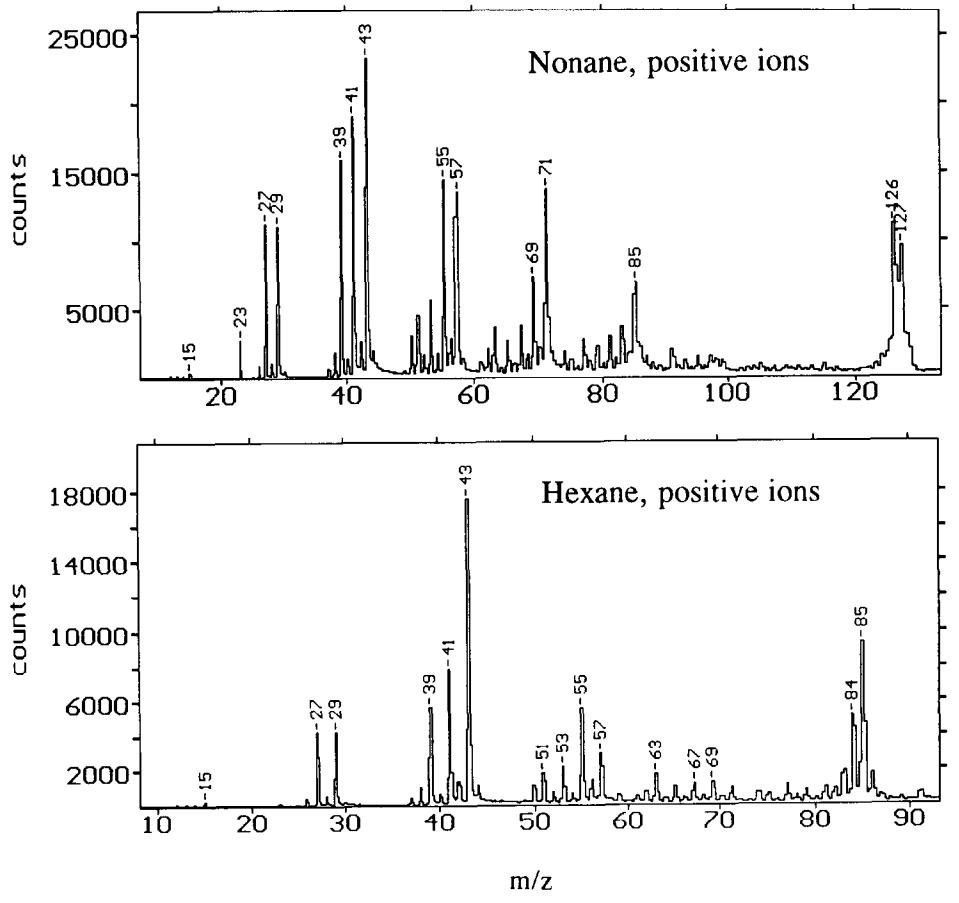

Fig. 1. Positive ion spectra of nonane and hexane.

2×10^{-3} mol l^{-1} benzene solution on an aluminized polyester foil using an air-brush-like apparatus.

The mass spectra of the alkanes were measured at Darmstadt. Details of the experiments will be presented in a forthcoming paper [5]. In order to produce spectra of clean alkanes, the samples were continuously refreshed by blowing the gaseous alkanes on the cold (−180°C) Cu holder during the measurement.

3. Positive ions

3.1. Experimental results

The positive ion spectra of nonane and hexane are depicted in Fig. 1. Only the mass region of the molecular and fragment ions are shown. Several mass peaks are present in the molecular ion region, but with alkanes mainly $[M - H]^+$ and $[M - 2H]^+$ are obtained (m/z 127 and 126 or 85 and 84). The spectra show a lot of fragments which form groups according to the number of carbon atoms. The yield for C_1-fragments, containing just one carbon atom is very low in all cases. The C_{n-1}-fragment yield is also low. The C_2-, C_3- and C_4-fragments appear very clearly in the spectra dominated by the C_3-fragments. All these spectra show several cluster series in the range of higher masses not depicted in Fig. 1.

The positive ion spectra of β-carotene and fullerenes are presented in the upper parts of Figs. 2 and 3. The isotopic pattern of the large peaks at m/z 536 and 720 depicted in the insets of these figures show that the molecular mass peak is $[M]^+$ for the C_{60} compound and $[M + H]^+$ with a slight contribution of $[M]^+$ for β-carotene. The

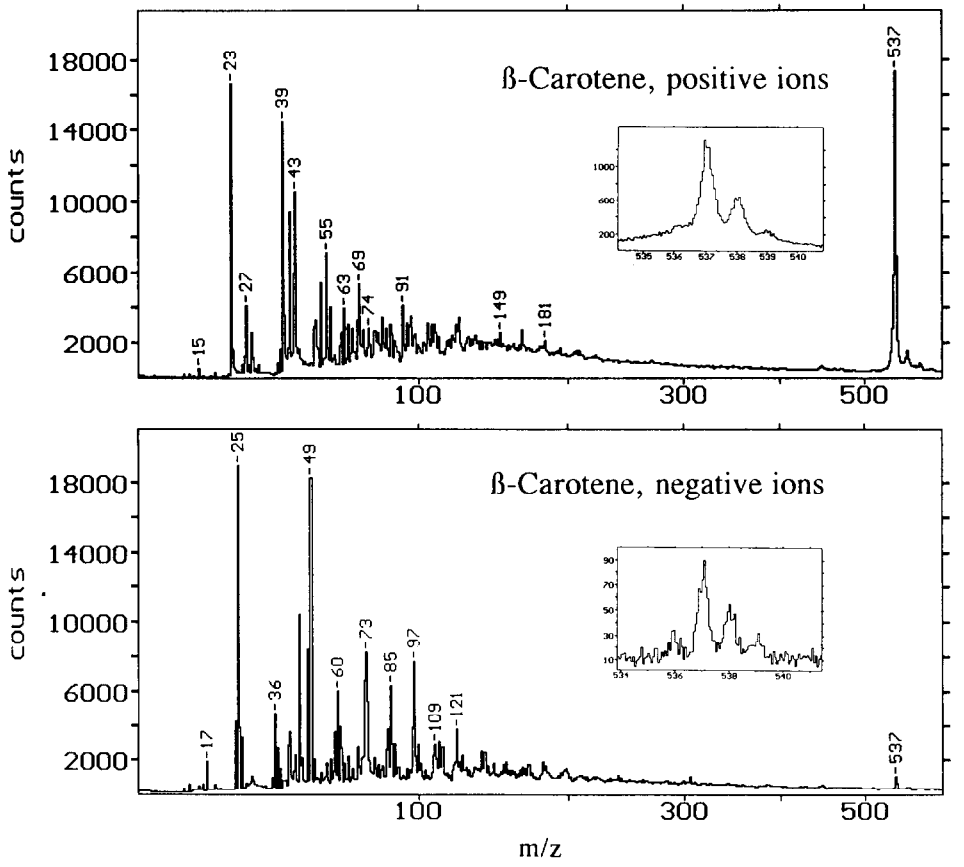

Fig. 2. Positive and negative ion spectra of β-carotene.

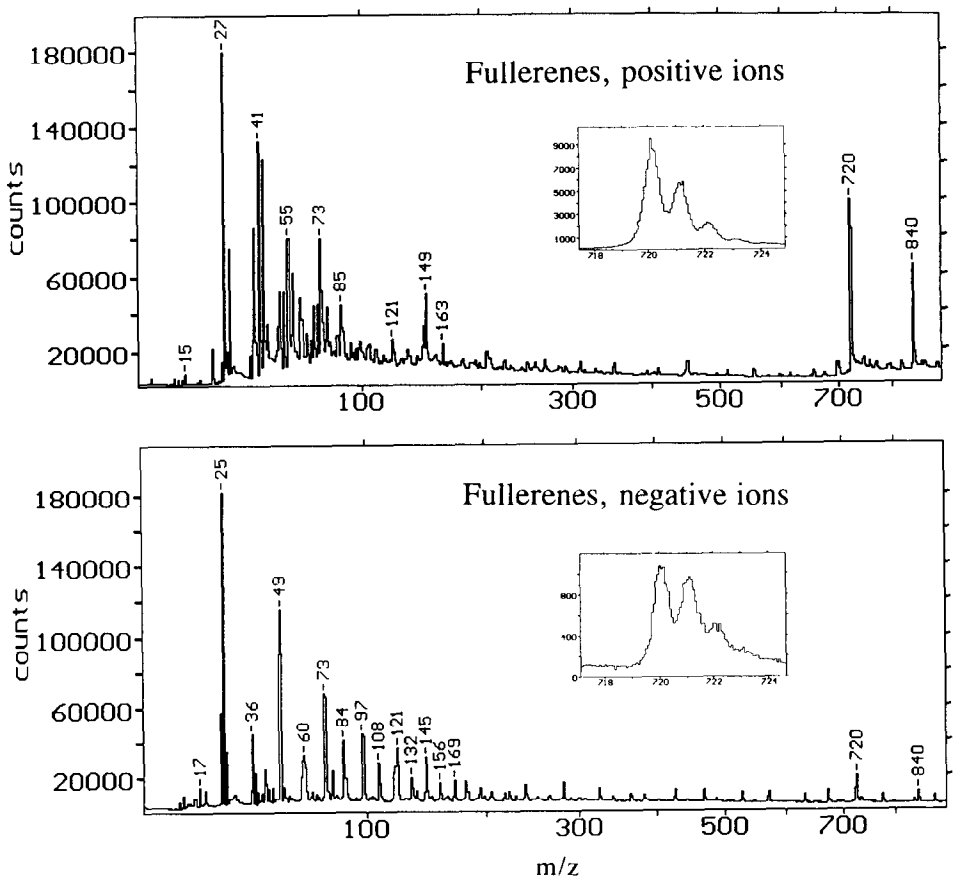

Fig. 3. Positive and negative ion spectra of fullerenes.

main fragments are C_2-, C_3-, C_4- and C_5-fragments in both spectra. The yields of the C_1-fragments are very low as for the alkanes. Nearly all mass lines depicted in the mass region of Fig. 3 between m/z 200 and 700 are members of Al_2O_3-cluster series. There are also small lines at m/z 720 ± 24 which are explained by the presence of small amounts of other carbon cluster compounds. The C_{70}-compound gives rise to a large peak at m/z 840. There are small peaks on the high mass side of the molecular ion peak of β-carotene (Fig. 2) arising from a few molecular ions which contain one or two additional oxygen atoms.

In general, all these positive ion spectra show:

(i) conspicuous molecular ion peaks;

(ii) low mass fragment ions with various intensities;

(iii) clusters of molecules.

3.2. Entropic fragmentation calculations

3.2.1. Introduction. The basic model scheme is that ions in ordinary PDMS-spectra stem from a large area around the primary ion track. The energy is transferred to the bonds by means of a secondary electron shower in a rather short time compared with thermal vibration times. Thus, the fragmentation here is thought to be mainly entropic, which means that probabilities for breaking chemical bonds should be almost independent for each bond of a molecule because of the high dE/dt value, so that there is no time to distribute the enormous amount of energy to other bonds before or during desorption, even within a single mole-

cule. This basic assumption is supported by the experimental observation that the kinetic energies of the desorbed molecules are in the order of the inverse of $\delta t/\hbar$, the expression one gains directly for the energy transformation time during the process from quantum mechanics perturbation calculations. The thermal energies, as measured, for example, by thermal fragmentation, are normally observed to be quite cold, i.e. about two orders of magnitude less than the above expression. Thus, the velocity of ions gives information on the initiating process time but contains no thermal information [9]. So the basic idea of the algorithm which we will describe below is to simulate this "entropic" resp. "independent" fragmentation mechanism.

3.2.2. CRUNCHER. The program CRUNCHER [6] assumes a statistically independent breakup of all chemical bonds of a given chemical structure of a molecule. The breakup probabilities are parameters which have to be fitted. The fit procedure [10] in the normally high-dimensional parameter space is undertaken by Monte-Carlo picking of start values and then locally exploring the maximum similarity to the experimental spectrum. For the similarity measure, several alternative measures (linear, quadratic ("Euclidean")) can be chosen. Great care has been taken to find effective algorithms to allow short enough computing times even for large molecules. Thus, CRUNCHER gives predictions of the abundances of mass lines by a sum of all fragmentation patterns of the molecule studied in terms of the purely adiabatic breakup. The program turned out to be very useful in predicting the numerous mass lines [11] of large molecules with known major breakup positions such as polypeptides, oligosaccharides, etc. In these molecules, however, the purely covalent bonds are relatively strong compared with, for example, glycosidic bonds so that they safely can be assumed to be small. Here, for the case of very light, simple, covalent bound atoms, where the hydrogen attachments and bonds determine the richness of the mass line groups, we tested the usefulness of the program in a limiting case.

CRUNCHER does not contain any information on the charge process. Thus it cannot predict any ions. To compare its results with an ion spectrum one has to assume a charging mechanism which keeps the ratio of fragment abundances. However, from the differences of a Crunch-spectrum to an experimental spectrum one may learn about the ionization mechanism, as well as on the validity of the basic assumption of the program that the breakup is purely entropic (in contrast to the thermal breakup as known, for example, with electron impact spectra).

A breakup of a molecule may be assumed to be accompanied by a charge separation onto the two resulting fragments; alternatively, in the case to be studied here, the charge could be picked by collisions with H_2 and H, prevalent in the expanding cloud. This mechanism may be supported by the finding that the respective negative fragment ions are not present.

3.2.3. Calculations for alkanes. We applied the program CRUNCHER to hexane and nonane, fitting to the experimental positive ion spectrum. In contrast to some large molecules such as polysaccharides, the experimental spectrum of hexane shows a lot of fragmentation lines indicating a large amount of internal energy deposited. The reference data for the fit were taken from the experimental spectrum by applying the peak-finding program PEAKS as described in detail in ref. 6. This allows the extraction of characteristic mass line data such as content and position by a fast and efficient algorithm. Then the experimental lines with the same carbon content were summed. The results for these fragment series $C_\nu H_\mu$ summing over all μ are given in Figs. 4(a) and 5(a) for hexane and nonane.

The bond-breakup probabilities of the covalent C–C bonds were the input data of CRUNCHER to produce the fragments of hexane. We then tried several different hypothetical bond structures for the carbon-backbone covalent bond chain. In Figs. 4 and 5 we give the results of the fit done with various assumed bond structures. We tested

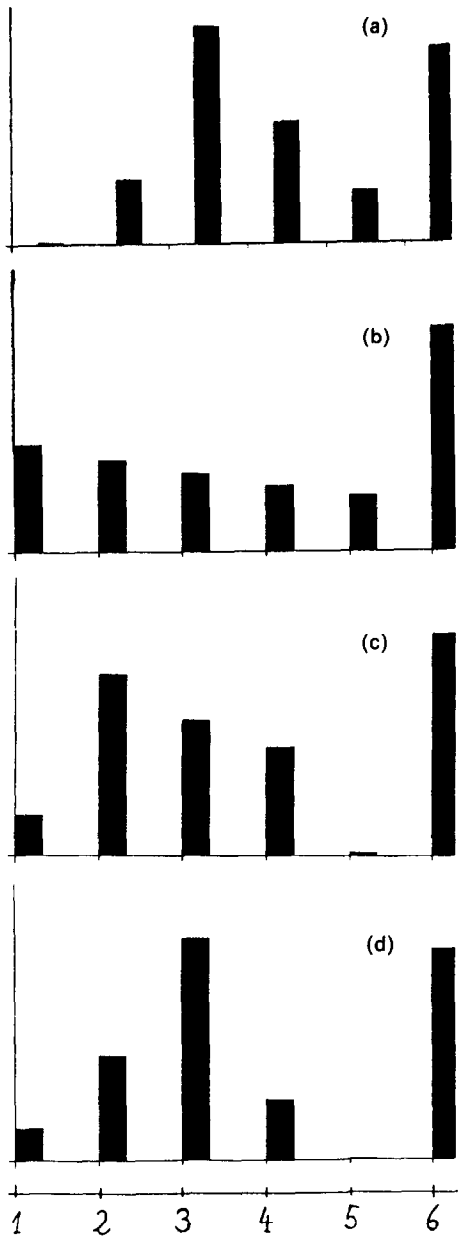

Fig. 4. Positive hexane spectrum with H-summed C_i fragments. (a) Experimental data. CRUNCHER-fit for the following assumed C–C bond strengths: (b) one type; (c) stronger end-bonds; (d) three central-symmetrically arranged bond types.

the following bond arrangements:

(i) just one type of bond was assumed, having in mind the chemical structure formula (Fig. 4(b));

(ii) two different bond types was assumed, the chain-end bonds being allowed to be stronger (Fig. 4(c));

(iii) a symmetric bond structure was assumed which gives a three parameter fit; this would be expected to simulate the preferred breakup if it was purely thermal (Fig. 4(d));

(iv) an alternating bond type (acetylenic structure) was tried; this could be proposed if one thinks that the hydrogen should be released as H_2 as known from polymer carbonization (slow thermal degradation) prior to desorption; but this gave an ill defined fit with no improvement against a simple one parameter fit.

For nonane we tested the following bond arrangements by fitting their bond strengths (see Fig. 5):

(i) just one type of bonds was assumed (Fig. 5(b));

(ii) an alternating "acetylenic" bond structure was assumed (Fig. 5(c));

(iii) a "thermal" bond arrangement was assumed, every third bond being allowed to be different (owing to the symmetry of nonane being different to hexane) (Fig. 5(d));

(iv) a chain but with stronger end-bonds was assumed (Fig. 5(e));

(v) a symmetric bond structure but in addition with stronger end-bonds (three parameter fit) was assumed (Fig. 5(f));

(vi) we did a full four parameter fit for a central-symmetric bond arrangement (Fig. 5(g)).

The quantitative results of the fits with regard to the respective breakup-probabilities w_i and to the similarity measure d are given in Table 1.

Finally, we skipped the experimental C_1 and C_2 fragments to enter the comparison. We then adjusted the bond break up probability for the end-bond of the chain to be 0.115 and for the inner bonds to be 0.2 for hexane and 0.06 and 0.18 for nonane, respectively. Without any detailed further fit the CRUNCHER spectra given in Figs. 6 and 7, are obtained.

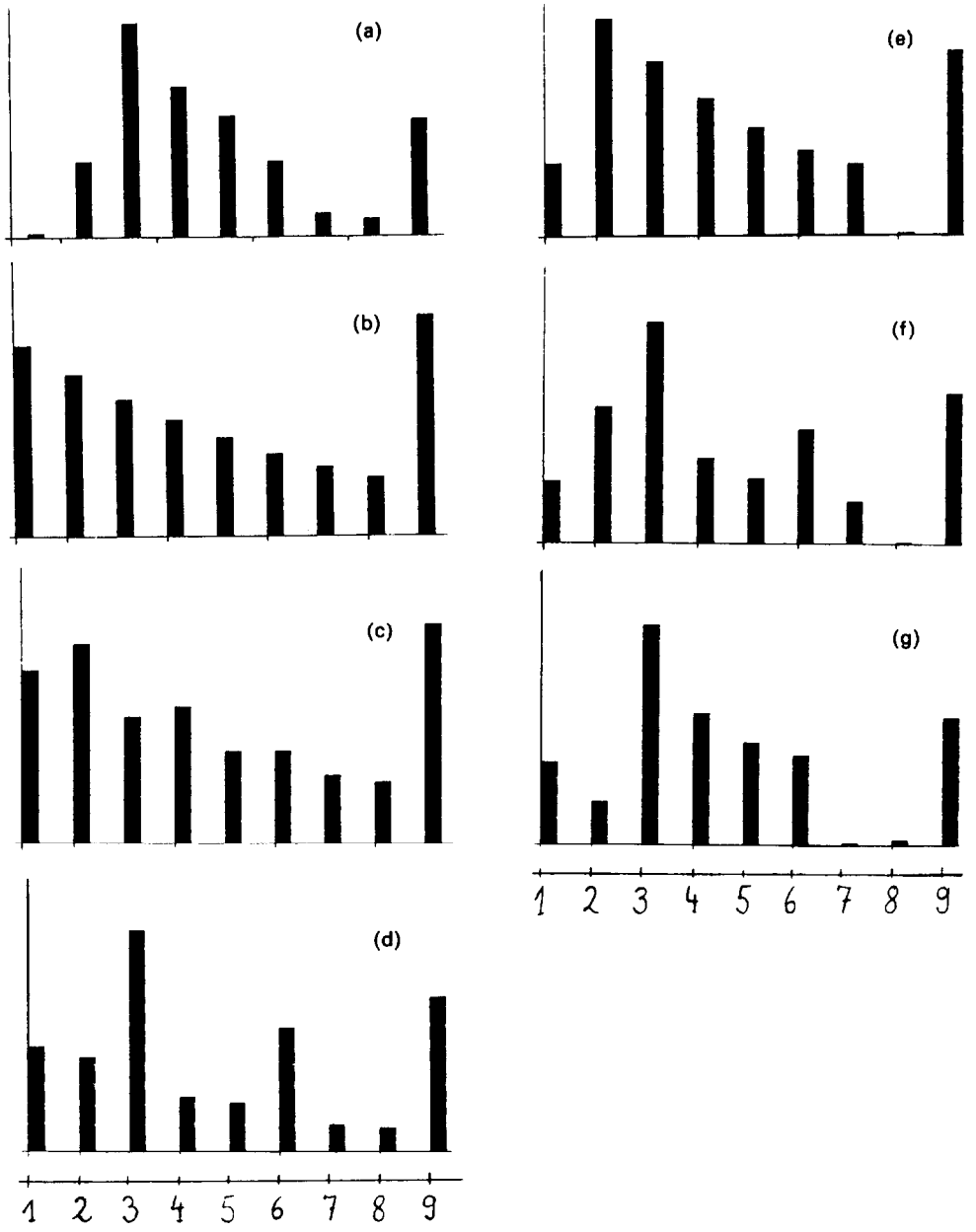

Fig. 5. Positive nonane spectrum with H-summed C_l fragments. (a) Experimental data. CRUNCHER fit for the following assumed C–C bond strengths: (b) one type; (c) alternating bond types (acetylenic); (d) two bond types, each third one stronger ("thermal"); (e) stronger end-bonds; (f) three bond types, symmetric but with stronger end-bonds; (g) four bond types, central symmetric arranged.

3.3. Discussion

We conclude that, most likely, the assumption of a purely entropic breakup is valid, that is, that the breakup process takes place in a time short compared with an inner-molecular thermal equilibration time, and, thus at the desorption. We attribute the lack of the smallest fragments, C_1 and C_2, to a later-stage collision neutralization. An acetylenic structure assumption is supported

Table 1A
Breakup probabilities w_i and similarity measures d to the experimental data: hexane

Bond type[a]	d	w_1	w_2	w_3	w_4
One type	0.82	0.110	–	–	–
Stronger end bonds	0.89	0.007	0.194	–	–
Symmetrical	0.96	0.001	0.127	–	–
Acetylenic structure	0.82		Ill defined fit		

Table 1B
Breakup probabilities w_i and similarity measures d to the experimental data: nonane

Bond type[a]	d	w_1	w_2	w_3	w_4
One type	0.782	0.11	–	–	–
Acetylenic	0.787	0.039	0.193	Mirror symmetric	
Every third bond stronger	0.922	0.0038	0.1181	–	–
Stronger end bonds	0.887	0.0036	0.1612	–	–
Stronger end bonds; symmetric structure	0.922	0.0038	0.1173	0.2463	–
Central symmetric structure	0.958	0.021	0.003	0.256	0.222

[a]For full details, see text.

by the experimental observation [12] that the spectrum reveals a strong H_2 detachment with regard to the hydrogen-number substructure, which probably serves to reduce the internal energy.

However, in the case of hexane and nonane this assumption leads to a result for the fit to the experimental spectrum, which is despite its two parameters (two bond types assumed) not at all better than the fit with just one parameter. We thus conclude that in PDMS the desorption does not take place by breaking up a preformed acetylenic structure one would get after detachment of hydrogen, the detachment of most of the hydrogen occurs *after* the desorption.

The fits seem to show that the end groups are less likely to break and that a symmetric fit is preferred. This would hint at a thermal component in the breakup. However, in performing the fit and leaving off the smallest two lines, we see that the fit is excellent with just a purely entropic breakup assumption of equal breakup probabilities for all bonds. We tend to the latter interpretation: a cold

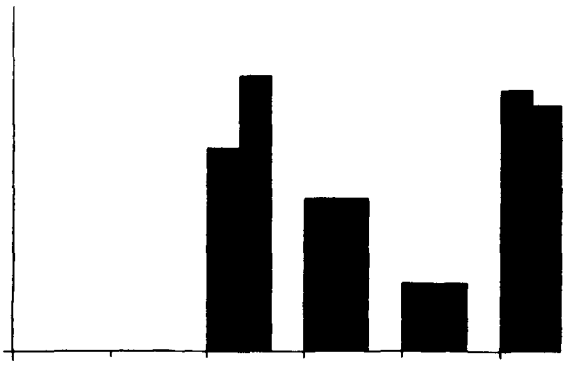

Fig. 6. CRUNCHER spectrum (left bars) as compared to the experimental data (right bars) of hexane.

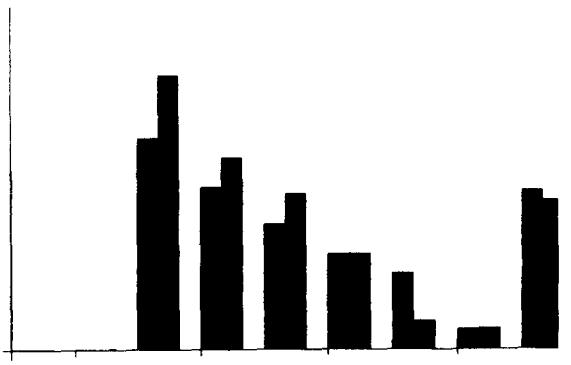

Fig. 7. CRUNCHER spectrum (left bars) as compared to the experimental data (right bars) for nonane.

entropic breakup of the original chemical structure and subsequent neutralization of the smallest fragment ions due to their high mobility and thus collision probability and also due to their reactivity. Simultaneously, the larger fragments detach their internal energy by H_2 detachment and thus "carbonize".

Comparing the results we see that the experimental finding of the very small amounts of $\nu = 1$ and $(n-1)$ lines, with $\nu = n/2$ being the maximum, cannot be quantitatively explained by any of these assumptions. We thus think that the ionization process leading to positive hydrocarbon fragments has to be revisited, for example, assuming post-desorption collisions in the plume, which might lead to neutralizations of initially ionized fragments as well, especially for the light and most reactive ones.

However, only positive ions of the molecules are observed, whereas in the negative spectrum these are missing. Thus, although we have calculated what an entropic breakup calculation would give for the examples chosen here, the mechanism of ionization cannot be that simple. We think that these observations will be a wide open field for fast gas phase chemistry and future analysis [5,12]. In particular, the de-dihydrogenated molecular ions could be fragments of the observed molecular clusters with quite different fragmentation patterns.

Experiments should be undertaken, for example, with position-sensitive detectors, to confirm the hypothesis that the positive ion spectra have a large initial energy and are desorbed preferrably sideways, whereas the negative ions in the case studied here are slower and peaked to zero degrees [13]. The process of ionization for PDMS needs and deserves a much more subtle study.

4. Negative ions

4.1. Experimental results

Negative ion spectra of β-carotene and fullerene are presented in the lower parts of Figs. 2 and 3 (see above). Negative ion spectra of nonane and hexane are given in Fig. 8. For comparison, the β-carotene and fullerene spectra are included in this figure showing the same mass range (m/z 5–150) for all compounds studied here. The same set of carbon cluster compounds C_nH_x ($n = 1,2,3,\ldots$; $x = 0,1,2,\ldots$) are observed with all samples in this mass range and only a very few mass peaks do not belong to these series. In addition, all spectra show nearly the same intensity pattern, in particular a very distinct odd–even effect with regard to the number of carbon atoms n. This result is highly remarkable, because the molecular

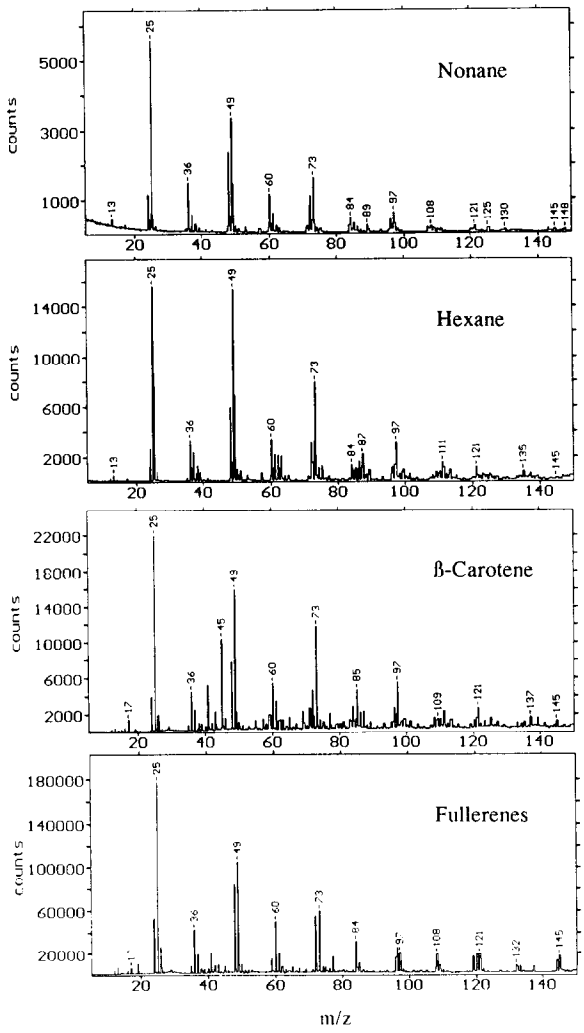

Fig. 8. Negative ion spectra from m/z 5 to 150.

size and structure of the compounds studied here are quite different.

Negative molecular ion peaks are completely absent in the case of nonane. The negative molecular ion peak of hexane might be among the peaks of the group ranging from m/z 84 to 89 in the hexane spectrum, but possibly it is also absent, as in the case of other alkanes [12].

There are clear negative molecular ion peaks of β-carotene and C_{60} (at m/z 537 and 720) but these are small if compared with the corresponding positive ones. The formation of these molecular ions may be due to the presence of small amounts of oxygen (see m/z 17 in Fig. 8 on the samples of these compounds). The β-carotene ions are observed as $[M+H]^-$, but $[M]^-$ is also slightly present. In contrast, the negative molecular ions of C_{60} are mainly $[M]^-$ with a slight contribution of $[M+H]^-$ (see isotopic pattern in the inset of Fig. 3). In both spectra, there is no clear indication of negative fragment ions of β-carotene and C_{60}. The region of low mass fragments is obviously dominated by the C_nH_x series. The negative peaks in the fullerenes spectrum between m/z 250 and 900 belong to the Al_2O_3-cluster series and the one at m/z 840 represents the negative molecular ion peak of the C_{70} compound.

In general, the negative ion spectra are obviously different as compared with the positive ones:

(i) the negative molecular ion peaks are small or completely absent;

(ii) there is a conspicuous set of negative ions easily assigned as C_n with eventual addition of only a few hydrogens;

(iii) very few negative mass peaks can be interpreted as fragment ions which are counterparts of those known from the respective positive ion spectra.

4.2. Adiabatic expansion model

The observed negative ion spectra are believed to be dominated by matter emerging from the ion track. One support for this is the absence of molecular ion peaks in the negative ion spectra. We identify three different series of carbon cluster compounds in the spectra:

(i) an even n-series of C_2, C_4, C_6, ...,
(ii) a series of C_2H, C_4H, C_6H, ...,
(iii) an odd n-series of C_3, C_5, C_7, ...

We have calculated the relative abundances of these three series and compared these with those taken from the experimental spectra. The similarity to the experimental abundance set of these carbon cluster series is striking (see Figs. 9–12).

Thus, we have obtained evidence for a process which is only dependent on the elements contained in the substance, but not on its molecular structure.

We give some reasons for the different abundances observed for the three series.

(i) the shape of the $C_{2n}H$-series is different from the other two because one of the possible C-sites is already blocked so that the probability of further attachment of carbons to the chain is decreased.

(ii) the C_{2n}-series has higher overall yields than the C_{2n+1}-series because the energy balance for the formation of the even chains is better, owing to a higher ratio of triple bonds, which are energetically favored in the formation process. In addition the even ones have a higher electron affinity [14].

The parameters of the calculations used to fit the experimental data are the initial matter density in the track prior to the incoming ion, which is well known, the initial temperature of the gaseous zone, which, however, drops out of the formulae owing to the adiabatic expansion assumed, and the sticking coefficient, which is known to be small and about constant. Thus, there is little to fit, which makes the model predictions so powerful and instructive [15].

Theoretically, we calculated the PDMS-abundance $f(n)$ for C_n for the ions coming from the innermost zone around the ion impact track by assuming a cylindrical area of hot, dense and completely atomized matter at the beginning of the expansion process, which is then followed by

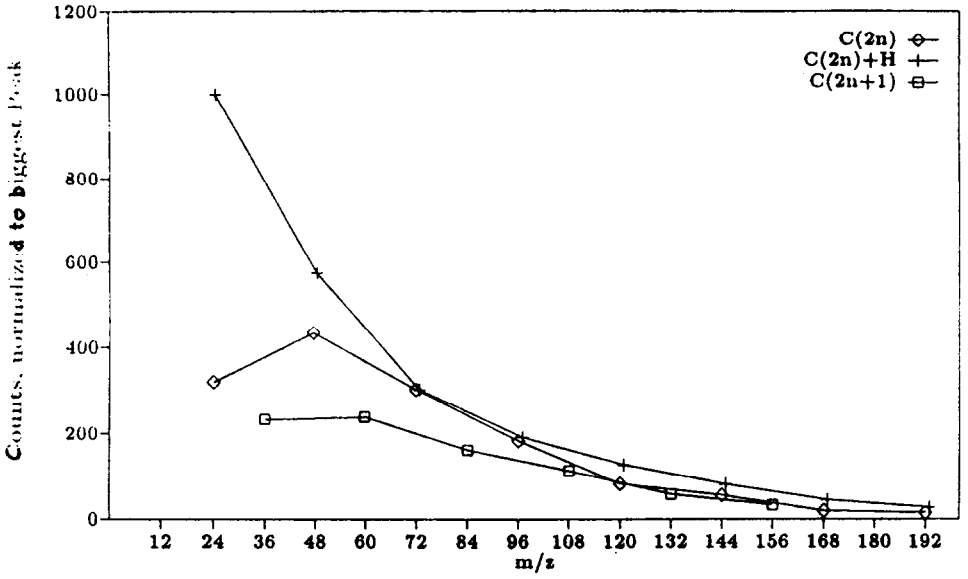

Fig. 9. Peak heights of negative ions extracted by the program PEAKS from the experimental spectrum of fullerenes.

an adiabatic expansion out of the primary impact hole. The sequential addition of carbon atoms during the expansion leads to carbon "clusters", the formation of which are stopped when the density of the expanding material becomes too low. Modeling the aggregation of carbon clusters we follow mathematically the adiabatic expansion of the material into a cone and track the abundance equation network of the carbon clusters. Here for simplicity and from experience we assume that the monomer (or dimer in this case) addition and detachment is dominating the cluster aggregation process. We thus skip the contributions of eventual cluster–

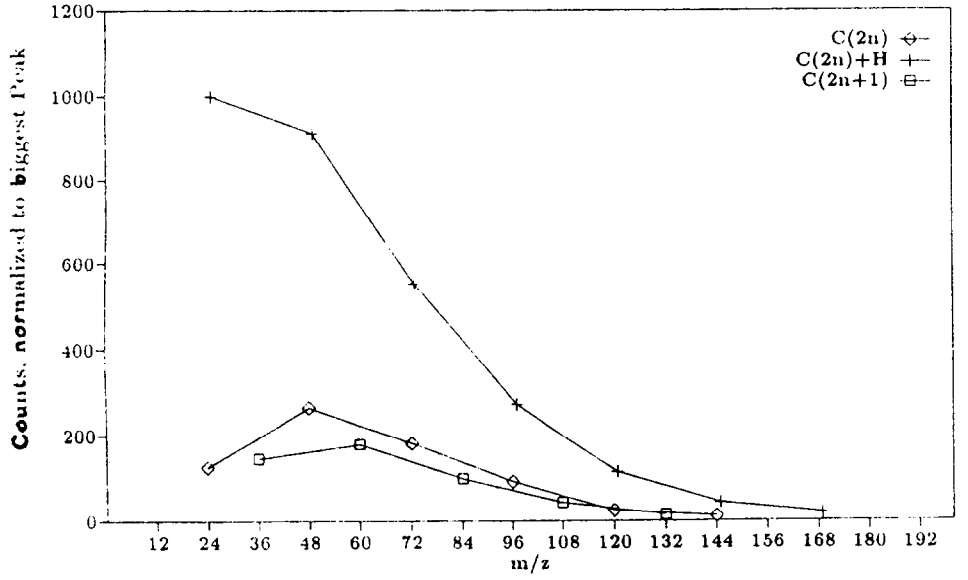

Fig. 10. Peak heights for negative ions extracted by the program PEAKS from the experimental spectrum of β-carotene.

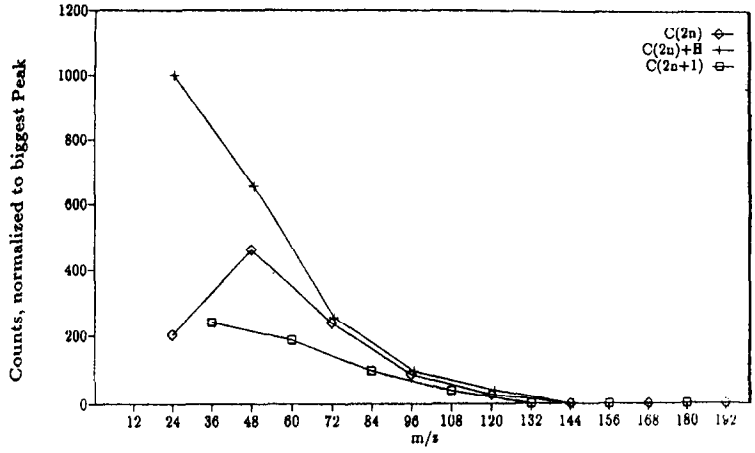

Fig. 11.Peak heights of negative ions extracted by the program PEAKS from the environmental spectrum of decane (as typical for alkanes).

cluster collisions. Going from an integral number of carbons n to a real variable, the advantage then is that we can simplify and analytically solve the network equations even on the adiabatically expanding gas environment (for the simple geometry of a cone). We end up with an analytical approximation expression [7]:

$$f(n) \approx n^{1/12} I_{1/4}(n^{2/3}\sigma^{-1}) \exp(-\tfrac{1}{2}n^{4/3}\sigma^{-1}) \qquad (1)$$

where σ is a thermohydrodynamical integral but proportional to the monomer sticking probability, which we take to be proportional to the

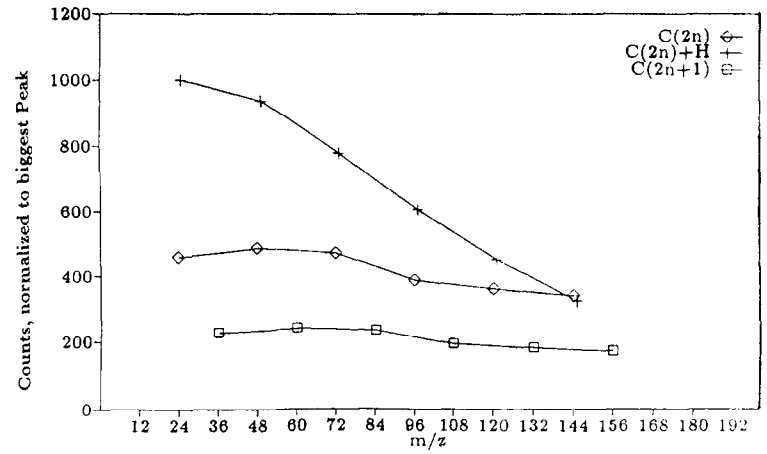

Fig. 12. Peak heights of negative ions as calculated by Eq. (1).

number of active ends of the molecule and the strength of the binding. We assume that the carbon clusters are actually polyydine-like chains. $I_{1/4}$ is the Bessel-Function of order one quarter. The function $C(\sigma)$ has been determined to be

$$C(\sigma) = \tfrac{2}{3} N_C \sigma^{-1} \exp^{-1/2\sigma^{-1}} \quad (2)$$

The absolute amplitude of the three cases was taken [16] to be 1:1/2:1/4 for $C_{2n}H$, C_{2n}, and C_{2n+1}, respectively. We are calculating these factors theoretically at the moment [15] together with a fully-fledged numerical calculation. We then hope to apply this algorithm to other related experiments such as the formation of fullerenes in desorption mass spectrometry [17,18]. $C(\sigma)$ is being calculated at the moment for different experimental settings.

4.3. Discussion

The observed set of carbon clusters are assumed to be acetylenic chains as known from polyydines C≡C–C. The set of carbon cluster series is about the same in all spectra, independent of what the original chemical structure of the molecule has been. This is emphasized by inspecting the spectrum of hexane, the lighter hydrocarbon, where one sees the same series which then reaches even far beyond the molecular mass. We are thus led to the conclusion that these clusters are formed by condensation subsequent to a complete destruction of the molecular structures. Energetically this can happen only in the area very close to the track of the impinging heavy ion.

As calculated in the fundamental thesis of Kammer [3] along the track right next to the path of the incoming ion, about 40 electrons per Ångström unit are set free. Thus, the atoms there are highly ionized and chemical structures with much lower binding energies are completely destroyed. As calculated by Kammer, the dense secondary electron cloud, blown into the surrounding solid, leaves a positively charged wake, which is then subsequently neutralized by the more slowly moving or slowed down part of the electrons. An estimate of the amount of neutralization may be inferred by inspecting the respective positive spectra. There are very little if not no positively charged C_n cluster lines.

The ions from the inner part of the track are often less prevalent in the mass spectrum for geometrical reasons: the ratio of radii of the inner part, where the deposited energy should be large enough to lead to a plasma (after the leaving of the secondary electrons, and thermalization), and of the total desorption zone is at most 10^{-1}, thus, the ratio of the respective surface areas should be less than 10^{-2}. Thus, if the surface density of desorbed ions were constant, they would be less prevalent by two orders of magnitude.

It should be mentioned that much earlier hints have been given to this part of the mechanism: it was noted that PDMS spectra look more like electron impact mass spectra, the higher the deposited energy density along the ion track is [19], that is, the higher the charge. In 1987, PDMS experiments on uranyl acetate gave the rather strange result that only uranyl-clusters were observed [20]. These results are now presently revisited in parallel with the present carbon cluster spectra.

5. Acknowledgements

One of us (E.R.H.) enjoyed stimulating and enlighting discussions with L. Pannell and H. Fales, W. Ens and K. Standing while at their laboratories. The creative and hospitable atmosphere at Gaspe greatly clarified the thinking in this field.

References

1 D.F. Torgerson, R.P. Skowronski and R.D. Macfarlane, Biochem. Biophys. Res. Commun., 60 (1974) 616.
2 D.F. Torgerson and R.D. Macfarlane, Science, 191 (1976) 920.
3 H.F. Kammer, Electronic Excitation in PDMS, PhD thesis, University of Oldenburg, (1991).
4 K. Wien. PDMS with volatile organic compounds, in K. Standing and W. Ens (Eds.), Methods and Mechanisms for Producing Ions from Large Molecules, NATO ASI Science series B, Vol. 269, Minaki, Canada, 1990, p. 27, 1991.

5 M. Wagner, K. Wien, B. Curdes and E.R. Hilf, Mass spectra of secondary ions ejected from frozen hydrocarbon gases by MeV ion impact, in P. Sigmund (Ed.), Fundamental Processes in Sputtering of Atoms and Molecules, Volume of Abstracts, SPUT92 Symposium, 30 August–4 September, 1992, Copenhagen, The Royal Danish Academy of Sciences and Letters, Copenhagen, 1992.
6 St. Harsdorf, E.R. Hilf, B. Nitzschmann, W. Schlez, F. Thomasdiewski, K. Koch and P. Wagner, Computer simulations, analysis and transfer of PDMS spectra, in W. Tuszynski and E.R. Hilf (Eds.), Mass Spectrometry of Large, Non-Volatile Molecules for Marine Organic Chemistry, International Workshops on the Physics of Small Systems, Vol. 3, World Scientific, Singapore, 1990, p. 164.
7 R. Böndgen, Bildung adiabatischer Cluster in adiabatischen Gasströmungen, Master's thesis, Technische Hochschule Darmstadt, (1985).
8 E.R. Hilf. PDMS and Clusters, in Lecture Notes in Physics, Vol 269, Springer, Berlin, 1987, p. 251.
9 E.R. Hilf. H.F. Kammer and B. Nitzschmann, Mechanisms of Desorption, in C.J. McNeal (Ed), The Analysis of Peptides and Proteins by Mass Spectrometry, Wiley, New York, 1988.
10 J. Curdes, P. Borrmann, E.R. Hilf and W. Tuszynski, Computer analysis tools for PDMS spectra, Proc. 40th ASMS Conference on Mass Spectrometry and Allied Topics, Washington DC, May 31–June 5, 1992, p. 567.
11 E.R. Hilf, Int. J. Mass Spectrom. Ion Processes, (1993) in press.
12 M. Wagner, K. Wien, B. Curdes and E.R. Hilf, Nucl. Instrum. Methods (1993) submitted.
13 R. Moshammer, PhD thesis, TH Darmstadt, Germany, (1991).
14 S.H. Wang, C.L. Petiette, J. Conceicao and R.E. Smalley, Chem. Phys. Lett., 139 (1987) 233.
15 B. Curdes, Cluster-Bildung Schwerionen-induzierter Desorption, Master's thesis, University of Oldenburg (1993).
16 B. Dohmen, J. Curdes, M. Wagner, E.R. Hilf, W. Tüszynski and K. Wein, Analysis of Entropic vs. Thermal Fragmentation, Proc. 40th ASMS Conference on Mass Spectrometry and Allied Topics, Washington, DC, May 31–June 5, 1992, p. 570.
17 G. Brinkmalm, D. Barofsky P. Demirev, D. Fenyo, P. Håkansson, R.E. Johnson, C.T. Reinmann and Bo. U.R. Sundquist, Chem. Phys. Lett., 191 (1992) 345.
18 M. May, Carbon clusters and fullerenes from carbon and platinum electrode materials, Proc. 40th ASMS Conference on Mass Spectrometry and Allied Topics, Washington, DC, May 31–June 5, 1992.
19 K. Wien, PDMS Introduction, in K. Wien, E.R. Hilf and H.F. Kammer (Eds.), PDMS and Clusters, Lecture Notes in Physics, Vol 269, Springer, Berlin, 1987, p. 1.
20 P. Weiland, K. Wien, S. DellaNegra, J. Deprauw, H. Joret and Y. Lebeyec, Cluster formation by fast heavy ion impact on metal acetates, in Y. Lebeyec, S. Della Negra and P. Thomas (Eds.), MeV and keV Ion and Cluster Interactions with Surfaces and Materials, Proc. 2nd International Workshop; Wangerooge Series of International Workshops on PDMS, Orsay, 1988, J. Phys. (Paris) Colloq. C, 2 (1989) 141.